Monophosphido-Bridged Early/Late Heterobimetallics: Synthesis, Structure, and Electrochemistry of $Cp_2Ti(\mu\text{-}PEt_2)(\mu\text{-}\eta^1\text{:}\eta^2\text{-}OC)M(CO)Cp$ (M = Mo, W)

David G. Dick, Zhaomin Hou, and Douglas W. Stephan*

Department of Chemistry and Biochemistry, University of Windsor, Windsor, Ontario, Canada N9B 3P4

Received January 28, 1992

The reactions of the Ti(III) species $[Cp_2Ti(\mu\text{-}PEt_2)]_2$ with $[CpM(CO)_3]_2$ (M = Mo, W) in benzene have been studied. The reactions proceed with reduction of the M–M bond and concurrent oxidation of the Ti(III) center to Ti(IV). The products are formulated as $Cp_2Ti(\mu\text{-}PEt_2)(\mu\text{-}\eta^1\text{:}\eta^2\text{-}OC)M(CO)Cp$ (M = Mo, **3a**: M = W, **3b**). The solvent dependence of these reactions is discussed. The compound **3a** crystallizes in the monoclinic space group $P2_1/c$ with a = 14.451 (8) Å, b = 9.703 (5) Å, c = 14.436 (6) Å, β = 102.93 (4)°, Z = 4, and V = 1986 (3) Å^3. The compound **3b** also crystallizes in the monoclinic space group $P2_1/c$ with a = 14.445 (6) Å, b = 9.674 (6) Å, c = 14.530 (4) Å, β = 103.22 (3)°. Z = 4, and V = 1977 (2) Å^3. The spectral, electrochemical, and structural characterization of these complexes are presented. Cyclic voltammetric studies of **3** show quasi-reversible reductions at −1.47 and −1.56 V for **3a** and **3b**, respectively. Chemical reduction of **3** with Na/Hg or $Na[C_{12}H_8]$ affords the extremely air sensitive complexes $Na[Cp_2Ti(\mu\text{-}PEt_2)(\mu\text{-}\eta^1\text{:}\eta^2\text{-}OC)M(CO)Cp]$ (M = Mo, **4a**; M = W, **4b**). The effect of oxidation state on the degree of CO activation is described, and the implications regarding heterobimetallic activation of CO are discussed.

Introduction

Our long-standing interest in complexes containing both early oxophilic and late electron-rich metals,[1] stems from the potential for carbon oxide activation and reduction. To this end, we have been pursuing systems in which only single bridging ligand links the two metal centers, thus offering a promising avenue for cooperative activation of carbon oxide substrates by the two metals. We have previously[2,3] described the synthetic routes to the monophosphido-bridged ELHB species of the form $Cp_2Zr(\mu\text{-}PR_2)(\mu\text{-}\eta^1\text{:}\eta^2\text{-}OC)Mo(CO)Cp$ (**1**) (R = Et, **1a**; R = Ph, **1b**) (Scheme I).

The two metal centers are held in close proximity by the bridging phosphide while the presence of the open coordination site on Zr permits Lewis acid activation of the carbonyl ligand bound to Mo.[2] In contrast, the initial attempts to prepare the analogous Ti species by employing the titanium(III) phosphide $[Cp_2Ti(\mu\text{-}PR_2)]_2$ proceeded with reduction of the Mo–Mo bond and oxidation of the phosphide ligand, yielding the Ti(III) species $Cp_2Ti(THF)(\mu\text{-}\eta^1\text{-}OC)Mo(CO)_2Cp$ (**2**).[3] These initial results seemed to imply that the relative redox potentials of Ti(III) and phosphide precluded the formation of monophosphido-bridged ELHB complexes containing Ti. These species are of particular interest as a result of the implication of the role of reduced Ti centers in strong metal-support interactions observed for heterogeneous catalyst systems.[4] This interest has prompted us to seek monophosphido-bridged ELHB species containing Ti. In this paper, we report the synthesis of such complexes. Chemical reductions of these compounds provide some insight as to the effect of oxidation state on cooperative CO activation. These results are described and the implications are considered.

Experimental Section

General Data. All preparations were done under an atmosphere of dry, O_2-free N_2 in a Vacuum Atmospheres inert-atmosphere glovebox. The atmosphere quality is maintained by employing a constant-circulation 5 ft^3/min purifier containing the Chemical Dynamics Corp. catalyst R3-11. Solvents were reagent grade, distilled from the appropriate drying agents under N_2 and degassed by the freeze–thaw method at least three times prior to use. ^1H and $^{13}C\{^1H\}$ NMR spectra were recorded on a Bruker AC-300 spectrometer operating at 300 and 75 MHz, respectively. Trace amounts of protonated solvents were used as references, and chemicashifts are reported relative to $SiMe_4$. $^{31}P\{^1H\}$ NMR spectra were recorded using a Bruker AC-200 NMR spectrometer operating at 81 MHz and are reported relative to 85% H_3PO_4 as an external reference. Infrared absorption data were recorded on a Nicolet 5DX Fourier transform IR spectrometer. Cyclic voltammetric experiments were performed by employing a BAS-CV-27 potentiostat. A platinum disk was used as the working electrode, a Ag/AgCl electrode was used as the reference, and Bu_4NBF_4 was used as the electrolyte. EPR spectra were recorded on a Varian E-12 EPR spectrometer, calibrated with an NMR gauss meter. The klystron frequency was determined from the EPR spectrum of DPPH. Combustion analyses were performed by Galbraith Laboratories Inc. Knoxville, TN, and Schwartzkopf Microanalytical Laboratories, Woodside, NY. Typical synthetic routes to complexes of the form $[Cp_2Ti(\mu\text{-}PEt_2)]_2$ have been previously described in the literature.[5] $[CpM(CO)_3]_2$ (M = Mo, W) was purchased from the Aldrich Chemical Co. PEt_2H was purchased from the Strem Chemical Co.

Scheme I. Synthetic Routes to the Monophosphido-Bridged Zr/Mo Species 1

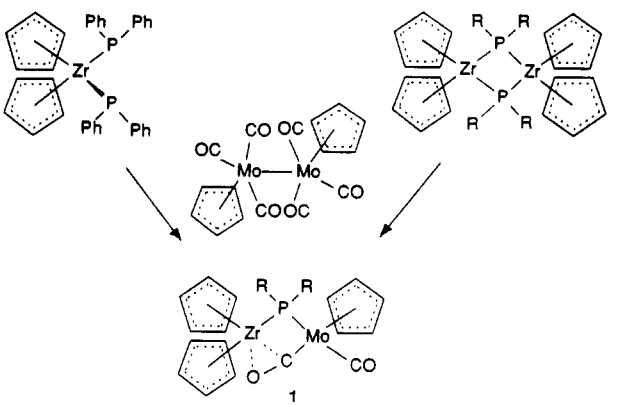

Synthesis of $Cp_2Ti(\mu\text{-}PEt_2)(\mu\text{-}\eta^1\text{:}\eta^2\text{-}OC)M(CO)Cp$ (M = Mo, 3a; W, 3b). To a benzene solution of $[Cp_2Ti(\mu\text{-}PEt)_2)]_2$ (0.036 g, 0.067 mmol) was added a benzene solution containing

(1) Stephan, D. W. *Coord. Chem. Rev.* **1989**, *95*, 41.
(2) Zheng, P. Y.; Nadasdi, T. T.; Stephan, D. W. *Organometallics* **1989**, *8*, 1393.
(3) Dick, D. G.; Stephan, D. W. *Organometallics* **1990**, *9*, 1910.
(4) Baker, R. T. K., Tauster, S. J., Dumesic, J. A., Eds. *Strong Metal-Support Interactions*; ACS Symposium Series 298; American Chemical Society: Washington, DC, 1986.
(5) Dick, D. G.; Stephan, D. W. *Can. J. Chem.* **1991**, *69*, 1146.

0276-7333/92/2311-2378$03.00/0

Table I. Crystallographic Parameters

	3a	3b
formula	$C_{21}H_{25}MoO_2PTi$	$C_{21}H_{25}O_2PW$
cryst color, form	orange-red blocks	red-black blocks
a (Å)	14.451 (8)	14.445 (6)
b (Å)	9.703 (5)	9.674 (6)
c (Å)	14.536 (6)	14.530 (4)
β (deg)	102.93 (4)	103.22 (3)
cryst syst	monoclinic	monoclinic
space group	$P2_1/c$ (No. 14)	$P2_1/c$ (No. 14)
vol (Å^3)	1986 (3)	1977 (2)
d_{calcd} (g cm^3)	1.62	1.92
Z	4	4
cryst dimens (mm)	0.43 × 0.38 × 0.44	0.40 × 0.38 × 0.54
abs coeff, μ (cm^{-1})	11.058	64.321
radiation, λ (Å)	Mo Kα (0.71069)	Mo Kα (0.71069)
temp (°C)	24	24
scan speed (deg/min)	8.0 ($\theta/2\theta$)	8.0 ($\theta/2\theta$)
scan range (deg)	1.0 below Kα1 1.0 above Kα2	1.0 below Kα1 1.0 above Kα2
bkgd/scan time ratio	0.5	0.5
no. of data collctd	3899	3883
2θ range (deg)	4.5–50.0	4.5–50.0
index range	$h,k,\pm l$	$h,k\pm l$
no. of data with $F_o^2 > 3\sigma(F_o^2)$	1885	1933
no. of variables	235	235
R (%)	4.11	4.32
R_w(%)	4.14	4.51
largest Δ/σ in final least-squares cycle	0.002	0.007
goodness of fit	1.086	1.169

$[CpMo(CO)_3]_2$ (0.033 g, 0.067 mmol). The mixture was stirred at room temperature for 18 h and then filtered. Addition of hexane into the benzene solution and standing overnight yielded red-orange crystals of **3a** (0.020 g, 0.046 mmol, 68% yield). Anal. Calcd for $C_{21}H_{25}MoO_2PTi$: C, 57.80; H, 5.78. Found: C, 57.70; H, 5.80. ^{1}H NMR (C_6D_6, δ, ppm): 5.23 (d, 5 H, $|J_{P-H}|$ = 1.7 Hz), 5.00 (s, 5 H), 4.94 (d, 5 H, $|J_{P-H}|$ = 1.5 Hz), 2.20 (m, 2 H), 1.83 (m, 2 H), 1.33 (dt, 3 H, $|J_{P-H}|$ = 14.2 Hz, $|J_{H-H}|$ = 7.4 Hz), 0.99 (dt, 3 H, $|J_{P-H}|$ = 13.0 Hz, $|J_{H-H}|$ = 7.3 Hz). ^{1}H NMR (THF-d_8, δ, ppm): 5.47 (d, 5 H, $|J_{P-H}|$ = 1.6 Hz), 5.34 (d, 5 H, $|J_{P-H}|$ = 1.0 Hz), 5.18 (s, 5 H). ^{13}C NMR (C_6D_6, δ, ppm): 236.1, 224.1, 106.1, 105.7, 88.8, 26.8 (d, $|J_{P-C}|$ = 7.0 Hz), 24.9 (d, $|J_{P-C}|$ = 12.0 Hz), 13.6 (d, $|J_{P-C}|$ = 7.0 Hz), 12.7 (d, $|J_{P-C}|$ = 5.0 Hz). ^{31}P{^{1}H} NMR (THF, δ, ppm): 218.0 (s). ^{31}P{^{1}H}NMR (C_6D_6, δ ppm): 182.0 (s). IR (THF, cm^{-1}): 1840, 1623. **3b.** Anal. Calcd for $C_{21}H_{25}WO_2PTi$: C, 48.11; H, 4.81. Found: C, 48.00, H, 4.80. ^{1}H NMR (C_6D_6, δ, ppm): 5.27 (d, 5 H, $|J_{P-H}|$ = 2.4 Hz), 4.95 (s, 5 H), 4.94 (d, 5 H), 2.40 (br m, 2 H), 1.85 (br m, 2 H), 1.30 (br m), 1.05 (br m). ^{1}H NMR (THF-d_8, δ, ppm): 5.41 (d, 5 H, $|J_{P-H}|$ = 1.5 Hz), 5.26 (d, 5 H, $|J_{P-H}|$ = 1.5 Hz), 5.20 (s, 5 H). ^{31}P{^{1}H} NMR (THF, δ, ppm): 178.9 ($|J_{W-P}|$ = 166 Hz). IR (THF, cm^{-1}): 1834, 1617.

Generation of Na[$Cp_2Ti(\mu$-$PEt_2)(\mu$-η^1:η^2-OC)M(CO)Cp] (M = Mo, 4a; W, 4b) (i) Na/Hg. A THF solution of **3a** was stirred over excess 1% Na amalgam for 18 h. During this period a color change from red-orange to green was observed. In the case of **4b**, exposure to the amalgam was limited to 0.5 h, as further reduction/decomposition was evident on prolonged exposures.

(ii) Na[$C_{12}H_8$]. A solution of a known concentration of sodium acenaphthalenide was prepared in THF. One equivalent of this reductant was added to THF solutions of **3**. In all cases, the reduced products **4** were characterized by both EPR and IR spectroscopy. These compounds were *extremely* air and moisture sensitive. All attempts to isolate these reduced materials failed, and ony the starting material products **3** were recovered. **4a.** IR (THF, cm^{-1}): 1742, 1671. EPR (THF): g = 2.002, $\langle a,^{31}P\rangle$ = 14.0 G, $\langle a,^{47/49}Ti\rangle$ = 10.0 G. **4b.** IR (THF, cm^{-1}): 1744, 1675. EPR (THF): g = 1.999, $\langle a,^{31}P\rangle$ = 18.0 G.

X-ray Data Collection and Reduction. Diffraction experiments were performed on a four-circle Rigaku AFC6 diffractometer with graphite-monochromatized Mo Kα radiation. The initial orientation matrices were obtained from 20 machine-centered reflections. These data were used to determine the crystal systems. An automated Laue symmetry check routine was employed to show that the crystal symmetries were consistent with monoclinic crystal systems.[6] Ultimately, 25 reflections ($20° < 2\theta < 35°$) were used to obtain the final lattice parameters and the orientation matrices. Machine parameters, crystal data, and data collection parameters are summarized in Table I. The observed extinctions were consistent with the space groups $P2_1/c$ in both cases. The data were collected ($4.5° < 2\theta < 50.0°$) and three standard reflections were recorded every 150 reflections. The intensities of the standards showed no statistically significant change over the duration of the data collection. The data were processed by use of the TEXSAN program package operating on a Vax 3520 workstation. The reflections with $F_o^2 > 3\sigma(F_o^2)$ were used in the refinement. An empirical absorption correction was applied to the data.

Scheme II. Synthetic Routes to 2 and 3

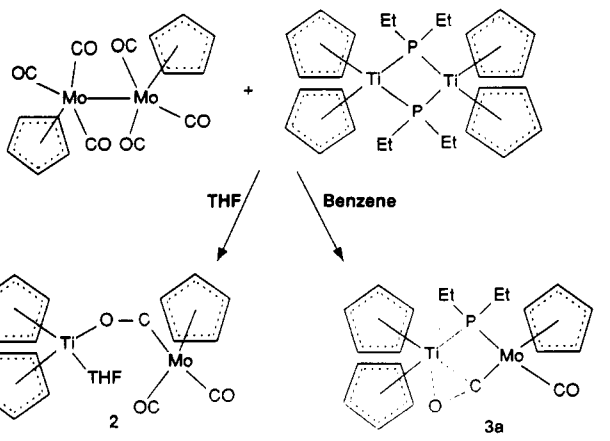

Structure Solution and Refinement. Non-hydrogen atomic scattering factors were taken from the literature tabulations.[6] The metal atom positions were determined using direct methods. The remaining non-hydrogen atoms were located from successive difference Fourier map calculations. The refinements were carried out by using full-matrix least-squares techniques on F, minimizing the function $w(|F_o| - |F_c|)^2$, where the weight, w, is defined as $4F_o^2/2\sigma(F_o^2)$ and F_o and F_c are the observed and calculated structure factor amplitudes. In the final cycles of refinement all the non-hydrogen atoms were assigned anisotropic temperature factors. Hydrogen atom positions were calculated and allowed to ride on the carbon to which they are bonded assuming a C–H bond length of 0.95 Å. Hydrogen atom temperature factors were fixed at 1.10 times the isotropic temperature factor of the carbon atom to which they are bonded. In all cases the hydrogen atom contributions were calculated but not refined. The final values of R and R_w are given in Table I. The maximum Δ/σ on any of the parameters in the final cycles of the refinement and the location of the largest peaks in the final difference Fourier map calculation are also given in Table I. The residual electron densities were of no chemical significance. The following data are tabulated: positional parameters (Table II) and selected bond distances and angles (Table III). Hydrogen atom and thermal parameters have been deposited as supplementary material.

Results and Discussion

The reaction of the Ti(III) dimer $[Cp_2Ti(\mu\text{-}PEt_2)]_2$[5] with $[CpM(CO)_3]_2$ (M = Mo, W) in THF was previously reported to yield the paramagnetic species $Cp_2Ti(THF)(\mu$-η^1:η^1-OC)$M(CO)_2Cp$ (**2**).[3] Similar reaction of $[Cp_2Ti(\mu\text{-}PEt_2)]_2$ and $[CpMo(CO)_3]_2$ in benzene does not yield the dark green product **2**; rather the reaction mixture gradually undergoes a color change from purple to orange-red over the period of 12–18 h, affording on workup a red-orange

(6) (a) Cromer, D. T.; Mann, J. B. *Acta Crystallogr. Sect. A: Cryst. Phys. Diffr. Theor. Gen. Crystallogr.* **1968**, *A24*, 324. (b) Cromer, D. T.; Mann, J. B. *Acta Crystallogr. Sect. A: Cryst. Phys. Diffr. Theor. Gen. Crystallogr.* **1968**, *A24*, 390. (c) Cromer, D. T.; Waber, J. T. *International Tables for X-ray Crystallography*; Kynoch Press: Birmingham, England, 1974. (d) Although cell reduction routines suggested the possibility of a orthorhombic *C*-centered lattice, axial photographs and Laue symmetry checks were not consistent with the higher symmetry.

Table II. Positional Parameters for 3a and 3b

atom	x	y	z
	Compound **3a**		
Mo(1)	0.25451 (5)	0.03116 (7)	0.45618 (5)
Ti(1)	0.33891 (3)	−0.1913 (1)	0.33383 (9)
P(1)	0.1762 (1)	−0.0695 (2)	0.3104 (1)
O(1)	0.4352 (3)	−0.1509 (5)	0.4770 (3)
O(2)	0.1520 (5)	−0.1756 (8)	0.5598 (4)
C(1)	0.3662 (5)	−0.0793 (7)	0.4755 (4)
C(2)	0.1910 (6)	−0.100 (1)	0.5192 (6)
C(3)	0.0655 (5)	−0.1676 (8)	0.3054 (6)
C(4)	−0.0137 (6)	−0.080 (1)	0.3261 (8)
C(5)	0.1318 (5)	0.0522 (8)	0.2116 (5)
C(6)	0.0792 (7)	−0.010 (1)	0.1180 (6)
C(11)	0.3945 (7)	−0.185 (1)	−0.1909 (6)
C(12)	0.4723 (6)	−0.171 (1)	0.2643 (7)
C(13)	0.4657 (6)	−0.046 (1)	−0.3087 (6)
C(14)	0.3808 (7)	0.0148 (8)	0.2631 (6)
C(15)	0.3383 (6)	−0.072 (1)	0.1897 (6)
C(21)	0.2353 (6)	−0.3833 (8)	0.2998 (7)
C(22)	0.2603 (6)	−0.3708 (8)	0.3989 (6)
C(23)	0.3552 (6)	−0.3993 (7)	0.4291 (5)
C(24)	0.3919 (6)	−0.4268 (8)	0.3510 (6)
C(25)	0.3166 (7)	−0.4190 (8)	0.2712 (6)
C(31)	0.3286 (7)	0.242 (1)	0.501 (1)
C(32)	0.272 (2)	0.265 (1)	0.411 (1)
C(33)	0.182 (1)	0.250 (1)	0.419 (1)
C(34)	0.179 (1)	0.220 (1)	0.508 (2)
C(35)	0.268 (1)	0.215 (1)	0.5579 (7)
	Compound **3b**		
W(1)	0.75489 (4)	0.03079 (6)	0.45709 (4)
Ti(1)	0.8391 (2)	−0.1925 (3)	0.3346 (2)
P(1)	0.6762 (3)	−0.0695 (4)	0.3111 (3)
O(1)	0.9360 (7)	−0.151 (1)	0.4746 (6)
O(2)	0.652 (1)	−0.175 (2)	0.5614 (9)
C(1)	0.867 (1)	−0.081 (1)	0.475 (1)
C(2)	0.694 (1)	−0.099 (2)	0.521 (1)
C(3)	0.566 (1)	−0.167 (2)	0.309 (1)
C(4)	0.486 (1)	−0.078 (2)	0.327 (2)
C(5)	0.633 (1)	0.055 (2)	0.211 (1)
C(6)	0.579 (1)	−0.009 (2)	0.119 (1)
C(11)	0.837 (1)	−0.076 (2)	0.189 (1)
C(12)	0.893 (1)	−0.187 (2)	0.190 (1)
C(13)	0.973 (1)	−0.174 (2)	0.266 (1)
C(14)	0.967 (1)	−0.047 (2)	0.309 (1)
C(15)	0.881 (1)	0.012 (2)	0.264 (1)
C(21)	0.854 (1)	−0.404 (2)	0.430 (1)
C(22)	0.762 (1)	−0.373 (2)	0.400 (1)
C(23)	0.737 (1)	−0.384 (2)	0.301 (1)
C(24)	0.817 (1)	−0.417 (2)	0.272 (1)
C(25)	0.894 (1)	−0.427 (2)	0.351 (1)
C(31)	0.682 (2)	0.245 (2)	0.421 (2)
C(32)	0.679 (2)	0.219 (2)	0.512 (2)
C(33)	0.772 (2)	0.214 (2)	0.562 (1)
C(34)	0.827 (1)	0.242 (2)	0.503 (2)
C(35)	0.773 (2)	0.261 (2)	0.411 (2)

microcrystalline solid. Monitoring of the reaction by $^{31}P\{^1H\}$ NMR showed the appearance of a peak at 218.0 ppm attributable to the new species **3a** (Scheme II). The NMR spectrum of **3a** shows ^1H resonances at 5.23, 5.00, and 4.94 ppm and $^{13}C\{^1H\}$ resonances at 106.1, 105.7, and 88.8 ppm, which are attributable to three inequivalent cyclopentadienyl groups. In the ^1H NMR spectrum, coupling of the cyclopentadienyl protons to a single phosphorus nucleus is evident. The two downfield resonances are assigned to Ti-bound cyclopentadienyl groups while the upfield resonance arises from a cyclopentadienyl ligand on Mo. ^1H NMR data for **3a** also shows multiplets centered at 2.20, 1.83, 1.33, and 0.99 ppm attributable to the inequivalent methylene and methyl moieties of the ethyl substituents on phosphorus. IR absorptions at 1840 and 1623 cm^{-1} are assigned to terminal and briding carbonyl groups, respectively. These spectroscopic data, in addition to combustion analyses, are consistent with the formulation

Table III. Selected Bond Distances (Å) and Angles (deg)

3a		**3b**	
Mo(1)–P(1)	2.378 (2)	W(1)–P(1)	2.372 (4)
Mo(1)–C(1)	1.905 (8)	W(1)–C(1)	1.92 (1)
Mo(1)–C(2)	1.92 (1)	W(1)–C(2)	1.90 (2)
Mo(1)–C(av)	2.34 (1)	W(1)–C(av)	2.33 (2)
Ti(1)–P(1)	2.585 (3)	Ti(1)–P(1)	2.588 (5)
Ti(1)–O(1)	2.264 (5)	Ti(1)–O(1)	2.227 (9)
Ti(1)–C(1)	2.284 (7)	Ti(1)–C(1)	2.26 (1)
Ti(1)–C(av)	2.393 (8)	Ti(1)–C(av)	2.39 (2)
P(1)–C(3)	1.848 (7)	P(1)–C(3)	1.84 (2)
P(1)–C(5)	1.860 (7)	P(1)–C(5)	1.88 (1)
O(1)–C(1)	1.212 (8)	O(1)–C(1)	1.20 (2)
O(2)–C(2)	1.16 (1)	O(2)–C(2)	1.18 (2)
P(1)–Mo(1)–C(1)	96.8 (2)	P(1)–W(1)–C(1)	96.3 (4)
P(1)–Mo(1)–C(2)	88.3 (2)	P(1)–W(1)–C(2)	89.3 (5)
P(1)–Ti(1)–O(1)	113.3 (1)	P(1)–Ti(1)–O(1)	113.6 (3)
P(1)–Ti(1)–C(1)	82.5 (2)	P(1)–Ti(1)–C(1)	82.6 (4)
C(1)–Mo(1)–C(2)	92.1 (3)	C(1)–W(1)–C(2)	91.8 (7)
O(1)–Ti(1)–C(1)	30.9 (2)	O(1)–Ti(1)–C(1)	31.0 (4)
Mo(1)–P(1)–Ti(1)	80.36 (8)	W(1)–P(1)–Ti(1)	80.5 (1)
Mo(1)–P(1)–C(3)	118.8 (3)	W(1)–P(1)–C(3)	117.3 (5)
Mo(1)–P(1)–C(5)	116.1 (3)	W(1)–P(1)–C(5)	116.0 (5)
Ti(1)–P(1)–C(3)	121.6 (3)	Ti(1)–P(1)–C(3)	121.5 (5)
Ti(1)–P(1)–C(5)	122.6 (3)	Ti(1)–P(1)–C(5)	121.8 (5)
C(3)–P(1)–C(5)	98.7 (4)	C(3)–P(1)–C(5)	100.4 (6)
Ti(1)–O(1)–C(1)	75.4 (4)	Ti(1)–O(1)–C(1)	76.2 (7)
Mo(1)–C(1)–Ti(1)	99.5 (3)	W(1)–C(1)–Ti(1)	99.9 (5)
Mo(1)–C(1)–O(1)	172.7 (6)	W(1)–C(1)–O(1)	172 (1)
Ti(1)–C(1)–O(1)	73.7 (4)	Ti(1)–C(1)–O(1)	72.8 (8)
Mo(1)–C(2)–O(2)	177.5 (8)	W(1)–C(2)–O(2)	177 (2)

of **3a** as $Cp_2Ti(\mu\text{-}PEt_2)(\mu\text{-}OC)Mo(CO)Cp$. While most of these spectroscopic data are similar to those previously reported for **1**,[2] the IR stretching frequency attributable to the bridging carbonyl of **3a** is shifted by approximately 50 cm^{-1} compared to that of the Zr/Mo analogue **1**. Despite this, the presence of an η^1-η^2-carbonyl fragment similar to that in **1** was confirmed by X-ray crystallographic studies of **3a** and **3b** (vide infra).

Employing a similar methodology, the reaction of $[Cp_2Ti(\mu\text{-}PEt_2)]_2$ and $[CpW(CO)_3]_2$ affords the W analogue of **3a**, that is $Cp_2Ti(\mu\text{-}PEt_2)(\mu\text{-}\eta^1\text{:}\eta^2\text{-}OC)W(CO)Cp$ (**3b**). The spectroscopic characteristics of **3b** are similar to those of **3a**. It is not surprising that the substitution of W for Mo has a comparatively small effect on the ν_{CO} for the η^1:η^2-OC moiety (**3a**) 1623 cm^{-1}; **3b**, 1617 cm^{-1}). This suggests that the major factor effecting the C–O bond order in these complexes is the σ donation of the π electrons to the Lewis acidic, early metal center. This interpretation is also reflected in a comparison of **3a** and **1a**, where the superior Lewis acidity or oxophilicity of Zr(IV) to Ti(IV) has a dramatic effect on the ν_{CO} for the η^1-η^2-OC moiety (**3a**, 1623 cm^{-1}; **1a**, 1567 cm^{-1}).

The present results indicate a solvent dependence of the course of the reactions of $[Cp_2Ti(\mu\text{-}PEt_2)]_2$ and $[CpMo(CO)_3]_2$. In THF **2**[3] is isolated whereas in benzene **3a** is formed (Scheme II). This solvent dependence is not well understood, but must be related to relative redox potentials for Ti(III)/Ti(IV) and $-PR_2/P_2R_4$ redox couples in the two solvents. It may be that in the formation of **2**, coordinated THF molecules assist in the stabilization of Ti(III), thus facilitating oxidation of phosphide to P_2R_4. Interestingly, although **3a** does not form in THF, it is stable in THF once isolated from benzene.

Structural Studies. X-ray structural studies of **3a** and **3b** confirmed the above formulations. Selected interatomic distances and angles are given in Table 3. An ORTEP drawing of **3a** is shown in Figure 1.

The coordination spheres of the metal atoms in **3a** and **3b** can be considered pseudotetrahedral. The M–C distances in the Cp_2Ti and CpMo fragments in **3a**, and the

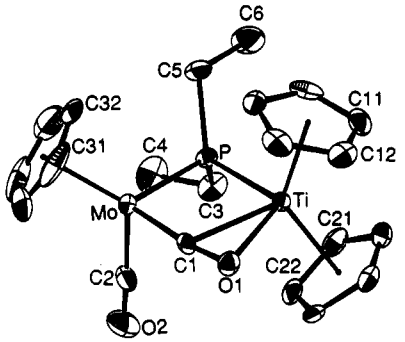

Figure 1. ORTEP drawing of molecule **3a**. Hydrogen atoms are omitted for clarity; 20% thermal ellipsoids are shown. Note that the number scheme for **3b** is identical with the substitution of W for Mo.

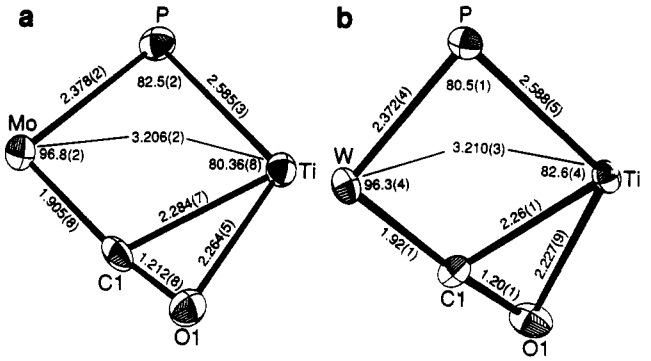

Figure 2. Structural details of the cores of **3a** and **3b**.

CpW fragments of **3b**, are as expected, as the M–C distances average 2.392 (8), 2.34 (1), 2.33 (2) Å, respectively. The bond distances within the terminal carbonyl and the bridging PEt_2 fragments are also quite typical and warrant no further comment.

The structural details of the cores of **3a** and **3b** are presented in Figure 2. In general, these structures are very similar to that previously described for $Cp_2Zr(\mu\text{-}PR_2)(\mu\text{-}\eta^1{:}\eta^2\text{-}OC)Mo(CO)Cp$.[2,3] The Ti–P distances of 2.585 (3) Å in **3a** and 2.588 (5) Å in **3b** are shorter than the Ti–P distances 2.606 (3)–2.631 (3) Å found in $[Cp_2Ti(\mu\text{-}PEt_2)]_2$.[5] This difference is consistent with the oxidation state of Ti. The Mo–P distance of 2.378 (2) Å observed for **3a** and the W–P distance of 2.372 (4) Å seen for **3b** are also significantly shorter than the corresponding distances found in $Cp_2Zr(\mu\text{-}Pr_2)(\mu\text{-}\eta^1{:}\eta^2\text{-}OC)Mo(CO)Cp$ (R = Et,[3] 2.401 (1) Å; R = Ph,[2] 2.417 (1) Å). The Ti–P–Mo and Ti–P–W angles of 82.5 (2)° and 80.5 (1)° found for **3a** and **3b**, respectively, are slightly greater than the corresponding angle of 79.8 (1)° foun in **1a**. The Mo–C(1) and W–C(1) distances of 1.905 (8) and 1.92 (1) Å found for **3a** and **3b**, respectively, are significantly longer than those of 1.876 (4) (R = Ph)[2] and 1.879 (4) Å (R = Et)[3] found in **1**. These structural data are consistent with a relatively weak M–C(1) bond compared to the analogous M–C(1) bonds in **1**. This implies a lesser degree of back-donation from Mo or W to the bridging CO in **3a** and **3b**. This is also consistent with the comparatively strong Mo–P or W–P bonds. The Ti–C and Ti–O bonds of the Ti(η^2-OC) fragment of **3a** and **3b** are 2.284 (7) and 2.26 (1), and 2.264 (5) and 2.227 (9) Å, respectively. These distances are comparable to those found in other ELHB species containing similar bound CO fragments such as $Cp_2Ti(\mu\text{-}CR)(\mu\text{-}\eta^1\text{-}\eta^2\text{-}OC)W(CO)Cp$[7] and

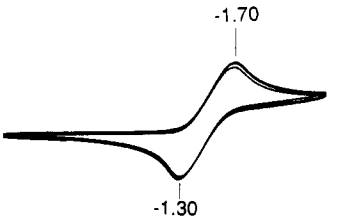

Figure 3. Cyclic voltammogram of **3a** in THF: scan speed, 200 mV/s; supporting electrolyte, Bu_4NBF_4.

Scheme III. Reduction of 3 to 4

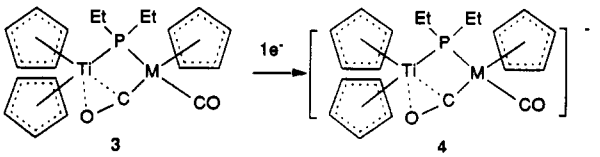

$Cp_2Ti(\mu\text{-}CRCH_2)(\mu\text{-}\eta^1{:}\eta^2\text{-}OC)W(CO)Cp$[8] The C–O bonds of these fragment are found to be 1.212 (8) and 1.20 (1) Å for **3a** and **3b**, respectively. These values are also similar to those observed for the Ti/M heterobimetallics that contain bridging $\eta^1{:}\eta^2$-carbonyl groups, reflecting substantial reduction in the C–O bond order compared to typical terminal carbonyl moieties. However, the present results are also consistent with the lower Lewis acidity of Ti compared to Zr. In **1**, the greater degree of C–O bond order reduction is evident in the C–O bond distance of 1.230 (5) Å as well as by the ν_{CO}.

The Ti–Mo and Ti–W separations of 3.206 (2) and 3.210 (3) Å in **3a** and **3b** are significantly shorter than those observed in **1** (3.243 (1), 3.250 (1) Å).[2,3] This reflects the smaller covalent radius of Ti. These metal–metal separations are substantially longer than in cases where a metal–metal bond has been confirmed. As was the case for **1**, these data suggest that metal–metal bonding is weak and support the zwitterionic formulation **3**.

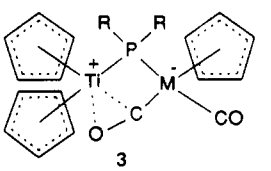

Electrochemistry. Compounds **3a** and **3b** were studied by cyclic voltammetry. In both cases the experiments were carried out in THF employing Bu_4NBF_4 as the supporting electrolyte, a Pt disk electrode, and a Ag/AgCl reference electrode. In the case of **3a**, a quasi-reversible reduction wave was observed at −1.47 V vs Ag/AgCl. The peak-to-peak separation was 400 mV (Figure 3). No other features were observed. In a similar fashion, **3b** also exhibited a quasi-reversible reduction wave at −1.56 V vs Ag/AgCl. The redox potential and the peak-to-peak separation suggest that these waves are due to a one-electron reduction centered at Ti. Similar Ti(IV)/Ti(III) redox couples have been observed in other heterobimetallic systems.[9]

Attempts to effect chemical reduction of **3a** and **3b** were made. In the case of **3a**, chemical reduction was effected by stirring a THF solution of **3a** over Na/Hg for 12 h, yielding **4a**. Analogous treatment of **3b** with excess Na/Hg for 12 h led to decomposition to an undefined phosphorus-based radical and other unidentified products. How-

(7) (a) Barr, R. D.; Green, M.; Howard, J. A. K.; Marder, T. B.; Moore, I.; Stone, F. G. A. *J. Chem. Soc., Chem. Commun.* **1983**, 746. (b) Dawkins, G. M.; Green, M.; Mead, K. A.; Salaun, J. Y.; Stone, F. G. A.; Woodward, P. *J. Chem. Soc., Dalton Trans.* **1983**, 527.

(8) Awang, M. R.; Barr, R. D.; Green, M.; Howard, J. A. K.; Marder, T. B.; Stone, F. G. A. *J. Chem. Soc., Dalton Trans.* **1985**, 2009.

(9) (a) White, G. S.; Stephan, D. W. *Organometallics* **1988**, *7*, 903. (b) White, G. S.; Stephan, D. W. *Organometallics* **1987**, *6*, 2169. (c) White, G. S.; Stephan, D. W. *Inorg. Chem.* **1985**, *24*, 1499.

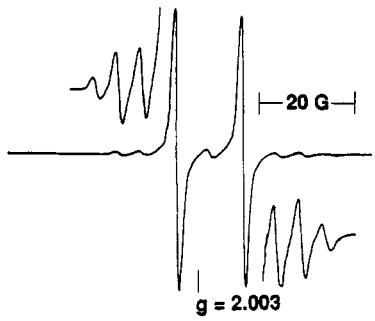

Figure 4. EPR spectrum of **4a** in THF at 25 °C.

ever, treatment of **3b** with excess Na/Hg for 20 min or treatment with a single equivalent of sodium acenaphthalenide yielded **4b** (Scheme III). All attempts to isolate these reduced species **4** failed, undoubtedly due to a extremely facile oxidation back to **3**. In fact, **3a** and **3b** were recovered quantitatively from such attempts. Nonetheless, the reduced species could be generated in small quantities for characterization. The reduction products **4a** and **4b** exhibited EPR spectra consisting of a center band doublet centered at $g = 2.002$ and $g = 1.999$ (Figure 4). These g values together with the observation of satellites attributable to $^{47/49}$Ti hyperfine confirm the formation of a formally Ti(III) species. The larger hyperfine couplings observed for the center band signal are attributable to coupling to the single phosphorus atoms. The coupling to phosphorus is significantly larger than that seen for $[Cp_2Ti(PEt_2)_2]^-$ ($g = 1.991$, $\langle a,^{31}P\rangle = 10.9$ G),[10] which is also in accord with the slightly greater g values in **4**. The IR spectra of **4a** and **4b** were similar showing bands at 1742 and 1671, and 1744 and 1675 cm^{-1}, respectively. These data lead to the formulation of **4a** as Na-[$Cp_2Ti(\mu$-$PEt_2)(\mu$-CO)M)CO)Cp]. Deliberate and short exposures of both the IR and EPR samples of **4** to air afford rapid and quantitative oxidation to starting materials **3**. The higher briding ν_{CO} of **4** are consistent with the population of an MO comprised largely of the LUMO on the Cp_2Ti molecular fragment.[11] The $1a_1$ orbital of the Cp_2Ti fragment is oriented in the direction of the bridging CO. Upon reduction to Ti(III), the degree of σ donation from the bridging CO to the Ti center is diminished. The nature of the bridging CO moieties in the reduced species is not known. It is noteworthy that a ν_{CO} of 1683 cm^{-1} is observed for $Cp_2Zr(\mu$-CO)(μ-η^1:η^2-OC)CoCp,[12] where the η^1:η^2 nature of the bridging CO has been crystallographically confirmed. However, the increase in the ν_{CO} of approximately 50 cm^{-1} upon reduction of **3** to **4** may also suggest a reorientation of the bridging group.

In summary, the titanocene(III) phosphide dimers react with the M–M bonded complexes $[CpM(CO)_3]_2$ (M = Mo, W) to yield monophosphido-bridged Ti(IV)/M products when the syntheses are done in benzene. These products are reducible, affording formally Ti(III)/M species in which CO bridges the two metal centers. The present compounds may be relevant to the study of mixed-metal heterogeneous catalysts in which the role of Ti(III) centers in the reactions of CO has been implied.[4] Efforts are underway to extend the synthetic methodology to related species in which both a reducible early metal and a catalytically active late metal are incorporated.

Acknowledgment. Financial support from NSERC of Canada is gratefully acknowledged. D.G.D. is grateful for the award of an NSERC of Canada postgraduate Scholarship.

Supplementary Material Available: Tables of hydrogen atom and thermal parameters for **3a** and **3b** (4 pages). Ordering information is given on any current masthead page.

OM9200464

(10) Dick, D. G.; Stephan, D. W. *Organometallics* **1991**, *10*, 2811.

(11) Lauher, J. W.; Hoffmann, R. J. *J. Am. Chem. Soc.* **1976**, *98*, 1729.

(12) Barger, P. T.; Bercaw, J. E. *J. Organomet. Chem.* **1980**, *201*, C39.